



Late production of Egyptian blue: synthesis from brass and its characteristics

Marco Nicola^{1,2} · Linda Marie Seymour³ · Maurizio Aceto⁴ · Emanuele Priola¹ · Roberto Gobetto¹ · Admir Masic³

Received: 9 March 2019 / Accepted: 23 May 2019 / Published online: 25 June 2019
© Springer-Verlag GmbH Germany, part of Springer Nature 2019

Abstract

This work follows the recent discovery of a zinc-bearing Egyptian blue (EB) pigment widely used for the production of the early medieval mural paintings cycle in Santa Maria *foris portas* Church at Castelseprio (Lombardy Region, Italy). The inclusion of zinc in the synthesis of EB has been studied for the first time trying to evaluate whether its addition could be casual or deliberate. Historical reconstructions of the pigment have been carried out with a special focus on the use of zinc besides copper, using the different production methods. The influence of zinc on the pigment's NIR photoluminescence and VIS-NIR reflectance has been characterized using FORS spectroscopy, X-ray diffraction, optical microscopy, and scanning electron microscopy-energy dispersive X-ray spectroscopy. A comparison of the production methods including salt-flux, solid-state, and Zn-rich syntheses showed that the solid-state synthesis results in particularly efficient NIR photoluminescence and VIS-NIR reflectance. Modern replicas were compared with an ancient sample in order to understand the zinc environment inside the structure of the Zn-enriched EB. Zn was found to be concentrated in a glass-based matrix surrounding cuprorivaite crystals, the main mineral associated with the EB pigment, and not included in a hypothetical Zn-doped cuprorivaite with formula $\text{CaCu}_{1-x}\text{Zn}_x\text{Si}_4\text{O}_{10}$. The Zn-rich synthesis opens up the possibility of producing EB from brass and demonstrates that EB used in Castelseprio's mural paintings could have been produced in this way. The relationship between the microstructure and the NIR photoluminescence of cuprorivaite-like pigments is of interest also for applications in modern and future technologies.

Keywords Egyptian blue · NIR photoluminescence · Zn-enriched cuprorivaite · FORS

✉ Maurizio Aceto
maurizio.aceto@uniupo.it

Marco Nicola
nicola@adamantionet.com

Admir Masic
masic@mit.edu

¹ Dipartimento di Chimica, Università degli Studi di Torino, Via P. Giuria, 7, 10125 Torino, Italy

² Adamantio S.r.l, Via G. F. Napione, 29/a, 10124 Torino, Italy

³ Department of Civil and Environmental Engineering, Massachusetts Institute of Technology, Cambridge, MA, USA

⁴ Dipartimento di Scienze e Innovazione Tecnologica (DiSIT) & Centro Interdisciplinare per lo Studio e la Conservazione dei Beni Culturali (CenISCo), Università degli Studi del Piemonte Orientale, Viale T. Michel, 11, 15121 Alessandria, Italy

Introduction

The Church of *Santa Maria foris portas* in Castelseprio is located almost 50 km northwest of Milan. Since 2011, it is listed in the UNESCO World Heritage Sites, as a part of the entry “Longobards in Italy: Places of the Power (568-774 A.D.)”. Inside the eastern apse of the church, there is an exceptional cycle of wall paintings depicting scenes from the Infancy of Christ taken from the Protoevangelium of James and from the Gospel of Pseudo-Matthew. Some scholars consider these paintings as a product of Western art, and others as an artwork belonging to a Byzantine Middle Eastern tradition. The different chronological attributions vary between the sixth and tenth century CE (Bertoni 2003). In 2013, the ante-quem term for the paintings has been more accurately established by the ¹⁴C wiggle-match dating (WMD) of the main timber beam,

dating the paintings between the end of the ninth and the first half of tenth century CE (Brogiolo 2013; Gheroldi 2013; Gheroldi 2017; Martinelli and Pignatelli 2013). One of the most important technical features concerning these paintings is the abundance of use of the pigment Egyptian blue (EB thereafter) (Nicola et al. 2018a) that is so widespread that seems unlikely (even if not impossible) that it could come from reuse of an older recycled pigment. In the recently published work (Nicola et al. 2018a) regarding the aforementioned cycle of paintings, the presence of a never-reported kind of zinc-rich EB (Cu:Zn about 4:1) was demonstrated, and a non-traditional manufacturing of EB using brass as a starting material was suggested. However, a precise knowledge of the raw materials, procedure, and conditions to produce that ancient pigment remains an open area of research. A similar kind of zinc-containing EB was very recently reported also on the fragments of painted plaster of analogous period, found in the Church of St. Philip in Hierapolis of Phrygia (Turkey) (Vettori S et al. 2019). EB containing minor amounts of zinc (0.5–1.2%) was also reported in other few archeological contexts (Ingo et al. 2013; Katsaros et al. 2010), but due to the limited amount registered, both Ingo et al. 2013 and Katsaros et al. 2010 stated that in those cases, it is more likely that zinc is present as a casual adding (e.g., a minor alloying element present in metals or ores used in the production). In modern applications, the presence of a zinc-containing cuprorivaite/gillespite is mentioned in US patent 2014/0072790 (Salguero et al. 2014) filed in concomitance with recent studies on EB and other metal–silicate nanosheet productions (Johnson-McDaniel et al. 2013; Johnson-McDaniel and Salguero 2014). Furthermore, zinc doping of cuprorivaite was studied by Li et al. (2014). Still, there is an inconsistency regarding the localization of Zn^{2+} ions within the structure. In the abovementioned patent (Salguero et al. 2014) indeed, Zn^{2+} is indicated as replacing the alkaline earth A^{2+} in the general formula $A_{1-x}C_xB_{1-y}D_ySi_4O_{10}$, where $A = Ca, Sr, \text{ or } Ba$; $C = Zn, Ti, \text{ or } \text{lanthanide element}$; $0 < x < 1$; $B = Cu, Cr, \text{ or } Fe$; $D = \text{alkali metal}$; $0 < y < 1$. A different conclusion was drawn by Li et al. (2014) stating instead that Zn^{2+} ions, due to similar ionic radius, are expected to be substituting for Cu^{2+} without changing the crystal field environment significantly (Li et al. 2014). Zn^{2+} is anyway seldom reported in square planar 4-fold coordination, as this geometry is unfavorable for Zn^{2+} which lacks the Jahn–Teller effect distortion that characterizes the Cu^{2+} ion (Greenwood and Earnshaw 1997). The research that is presented below is the most complete technical study of Zn incorporation into EB pigment. Regardless if the presence of zinc is intentional or unintentional both in ancient and modern samples, a description of zinc-bearing EB inner structure and the localization of Zn is important for the knowledge of historical

and modern production technologies and for a better conservation of this kind of pigments. Among other aspects, a special focus has been put on the effects of the presence of zinc on the characteristic NIR photoluminescence of EB. This feature can help to improve non-destructive characterization techniques and also is fundamental for modern and future applications of this kind of materials.

Egyptian blue history and structure

Used since the third millennium BCE (Riederer 1997) and before (Corcoran 2016), EB is considered the first true synthetic pigment (Riederer 1997). Its production is linked to the development of pottery and of materials such as Egyptian faience, glass, and bronze (El Goresy et al. 1996; Kaczmarczyk and Hedges 1983). The Egyptians called it *hsbd iryt*, which means *artificial lapis lazuli* (Giménez et al. 2017). It was by far the most common blue pigment in the ancient Europe, West Asia, and North Africa (Gaetani et al. 2004), but, after the collapse of the Western Roman Empire, it gradually disappeared (Riederer 1997). Quite seldom, occurrences are reported in the Middle Ages (Bensi 1990; Mairinger and Schreiner 1986; Lazzarini 1982; Lluveras et al. 2010; Nicola et al. 2018a) and exceptionally in Renaissance (Bredal-Jørgensen et al. 2011; Chiari 2018). The reasons why its use was abandoned are still debated (Gaetani et al. 2004).

At the beginning of nineteenth century, while searching for a cheap, deep-blue, inorganic pigment (Berke 2007), a new interest in EB arose. Some samples from Pompeii were studied in 1809 by Chaptal (1809) and in 1815 by Sir Humphry Davy (1815) making EB one of the first materials from antiquity to be examined by the modern scientific methods (Tite et al. 1984). Subsequently, many successful attempts to reproduce it were done (Riederer 1997; Warner 2011) by (1) scientists interested in trying to reproduce the ancient pigment for historical purposes, (2) technicians who wanted to reintroduce EB as a modern pigment, and (3) mineralogists who experimented with the synthesis of cuprorivaite to understand its crystallographic properties. To avoid confusion, in this work, the term “Egyptian blue” will refer to both archeological specimens and modern products obtained by artificial synthesis (containing also amorphous phases or other minerals different from $CaCuSi_4O_{10}$), while “cuprorivaite” will be used referring to the natural or artificial pure $CaCuSi_4O_{10}$ crystalline compound.

Cuprorivaite has a phyllosilicate structure described for the first time by Pabst (1959). It is analogous in structure to $SrCuSi_4O_{10}$ (wesselsite) and $BaCuSi_4O_{10}$ (effenbergerite), the latter being the main constituent of the ancient pigment Han blue (Johnson-McDaniel and Salguero 2014). All three minerals are members of the gillespite ($BaFeSi_4O_{10}$) group, having the form $ABSi_4O_{10}$ ($A = Ca, Sr, \text{ or } Ba$ and $B = Fe, Cu,$

or Cr) (Johnson-McDaniel and Salguero 2014; Salguero et al. 2014). The deep blue color of cuprorivaite, wesselsite, and effenbergerite is primarily due to the Cu^{2+} ion in square planar coordination (D4h) (García-Fernández et al. 2015). The exact color coordinates of EB are influenced also by particle dimensions (i.e., smaller particles make the pigment clearer) and by other factors such as the unbalance in the constituents and the presence of impurities (Hatton et al. 2008; Johnson-McDaniel and Salguero 2014; Riederer 1997). All three minerals have strong luminescence yield in the 800–1100 nm NIR region (Berdahl et al. 2018), with emission at ca 950 nm with increasing wavelength in the Ca, Sr, and Ba series (Chen et al., 2016) when excited with red light between 600 and 630 nm (Accorsi et al. 2009; Pozza et al. 2000; Verri 2009b). Their photoluminescence is based on the Cu^{2+} ion located on the fourfold axis, where it links four SiO_4 tetrahedra in a square planar coordination (Chiari 2018). The discovery of the near-infrared (NIR) photoluminescence of EB and related materials (Accorsi et al. 2009; Pozza et al. 2000; Smith et al. 2009) has led to several advancements in cultural heritage science (Dyer et al. 2013; Kakoulli et al. 2017; Verri 2009a, b) and in other disciplines such as optics (Borisov et al. 2013), nanotechnologies (Johnson-McDaniel and Salguero 2014; Salguero et al. 2014, Chen et al. 2016), and forensic science (Errington et al. 2016). The bacteriostatic effect of EB recently investigated is also promising in biomedicine (Tian et al. 2016). All these recent advancements increased the prospective of EB to be exploited as an outstanding paleo-inspired system (Bertrand et al. 2018).

The production of EB in ancient times was performed through a process of the salt-flux synthesis (Pradell et al. 2006), using fluxes such as plant ashes (Jaksch et al. 1983) or natron, a naturally occurring salt from salt lakes (e.g., Wadi El Natrun in Egypt) consisting mainly of $\text{Na}_2\text{CO}_3 \cdot 10\text{H}_2\text{O}$ (Etcheverry et al. 2001; Giménez et al. 2017; Riederer 1997; Shortland et al. 2006). Though it is more difficult to obtain due to higher temperature requirements, the solid-state synthesis was likely also possible in antiquity (Delamare 1997; Etcheverry et al. 2001); however, pigment obtained in this way is a pale blue instead of deep blue (Johnson-McDaniel and Salguero 2014). The archeological use of this kind of synthesis remains debated (Pradell et al. 2006). In archeology-inspired EB production during the nineteenth and twentieth centuries, a finely ground, almost stoichiometric (Johnson-McDaniel and Salguero 2014; Mazzocchin et al. 2004; Warner 2011) mixture (4:1:1) of SiO_2 , CaO (typically from CaCO_3), and CuO (from a copper-bearing material) was heated with a small amount of a flux (e.g., Na_2CO_3) to about 800–900 °C (Riederer 1997). Depending on the procedure, the temperature needed to be maintained for 10–392 h (Riederer 1997). The ancient recipe is described by Vitruvius in *De Architectura*, Book

VII, Chapter 11-1 (Vitruvius 1999). He describes that sand, probably containing both SiO_2 and CaCO_3 in the proper ratio (Mazzocchin et al. 2004), natron (flux), and filings of metallic copper were mixed with some water to create a paste and shaped in the form of small spheres. Such prepared spheres were then air dried and fired in terracotta vessels (Riederer 1997; Warner 2011).

There is some debate about the source of copper used for the production of ancient EB. Recent recipes generally use $\text{Cu}_2(\text{CO}_3)(\text{OH})_2$ (malachite) or CuO as a source (Johnson-McDaniel and Salguero 2014; Mazzocchin et al. 2004; Riederer 1997; Tite et al. 1984; Warner 2011). The direct use of copper ores such as malachite was probable in antiquity (Tite et al. 1984) due to the wide availability of that mineral (e.g., from copper mines in the Sinai desert). Vitruvius, however, mentions metallic copper filings (Warner 2011), and modern analysis of archeological EB and Egyptian Faience samples show a characteristic, univocal relationship between metallurgy development and sample composition (El Goresy et al. 1996; Kaczmarczyk and Hedges 1983; Nicola et al. 2018b). In ancient EB samples, it is possible to distinguish minor amount of elements likely derived from arsenical bronze (from the Ancient Kingdom to the middle of the fifteenth century BCE), Sn bronze (from 1479 to 1425 BCE), and on later samples Sn–Pb bronze (Fenoglio et al. 2012; El Goresy et al. 1996; Kaczmarczyk and Hedges 1983). Recently, the presence of considerable amount of Zn together with Cu in the Castelseprio EB suggests also the use of a copper/zinc alloy in late productions of EB, supporting this correlation (Nicola et al. 2018a). The alloy used can be identified with *orichalcum*, a famous ancient alloy normally considered to be a copper alloy containing a consistent amount of zinc (Caley 1964; Caponetti et al. 2017). Currently, this kind of alloy is termed brass. The concentration of zinc with respect to copper (in average 21.2%) is consistent with the values normally obtained with the cementation process that is the method of producing these alloys in antiquity (Bourgarit and Bauchau 2010; Caponetti et al. 2017).

Zinc-enriched EB

In this work, we explore the ancient Zn-enriched cuprorivaite-based technology in order to reverse engineering the material from direct, in-depth physico-chemical, morphological, and compositional analysis. The entire process includes the following steps: understanding the composition and structure of the ancient material, reverse engineering its production routes, and comparing the newly produced materials' properties with those of the ancient samples.

Experimental

Ancient Zn-rich Egyptian blue sample

The sample was a detached fragment picked up during the 2012 campaign of analyses (Nicola et al. 2018a). It came from the *Adorazione dei Magi* scene (Fig. 1) and more specifically from the blue decorative ribbon in the lower part of the painting. The sample was embedded in polyester resin and polished perpendicularly to the surface to obtain a cross section. The cross section was first abraded with carbon papers (800–1200 mesh) and then polished using diamond pastes (0.25 μm). The cross section was observed under different microscopes (see below for further details) and compared with powdered artificial samples embedded in polyester resin and polished in the same way.

Artificial samples

The artificial samples of EB were produced in a ceramic kiln WLF 2000 Light & Power regulated by a Pixsys ATR243 controller (see Fig. 2 left). Three powders of brass with a different ratio Cu:Zn were chosen to evaluate the effect of Zn concentration. An experimental archeology approach was used (Mathieu 2002), so the powders of brass were collected from true ancient brass object (see Fig. 2 top right). Before the synthesis, the brass used was characterized with SEM-EDS to accurately evaluate Cu:Zn ratio and to identify the presence of other elements.

As suggested by Mazzocchin et al. (2004) and Warner (2011), the main syntheses were carried out in self-made terracotta crucibles (shown in Fig. 2). The clay used to produce terracotta crucibles was purchased from Colorobbia and was of the quality “Argilla Rossa.” Prior to the syntheses, the crucibles were heated at 1000 °C for 12 h, naturally cooled down to 20 °C and accurately washed in water.

SiO₂ and CaCO₃ used were of commercial grade and were purchased from Chimica Strola in Turin. Prior to the synthesis, they were tested with SEM-EDS to check for detectable impurities (e.g., K and Al) that can play a role in the production process. They resulted with trace concentrations of those specimens, quite close to the detection limit. The other reactants (HCl, Na₂CO₃, CuO, and Cu metal) were purchased from Sigma-Aldrich (Milwaukee, USA). Commercial Egyptian blue was purchased from Kremer Pigmente (Aichstetten, Germany).

Physico-chemical characterization

Microscopy

Optical microscopy and scanning electron microscopy-energy dispersive X-ray (SEM-EDS) measurements were carried out



Fig. 1 The *Adorazione dei Magi* scene with the indication of the sample location

to characterize ancient and newly produced EB. For the optical microscopic analyses, a UV/optical microscope Olympus BX-41 was used, equipped with the fiber optic illumination system Optika Microscopes, UV lamp UV Olympus U-RFL-T and filter cube Olympus U-MWU (330–385 nm).

Different SEM-EDS instrument were used:

1. XVP-SEM ZEISS EVO 50 scanning electron microscope equipped with a microanalysis system (EDS) INCA Energy 250 (Oxford Instruments), using a lanthanum hexaboride (LaB₆) filament as electron source at 20 keV. It was used in variable pressure mode in order to avoid sample metallization (beam current, 200×10^{-12} A; pressure: 55 Pa; air type: room air; stub: aluminum (diameter 12.5 mm, sample attached with conductive carbon tape); quantification technique, semiquantitative analysis (INCA Suite version 4.14)).
2. Further SEM-EDS data were collected using a TESCAN RISE scanning electron microscope. All samples were imaged in low vacuum (30 Pa) with an acceleration voltage of 20 keV (beam current: 493×10^{-12} A; air type: N₂; stub: aluminum (diameter 12.5 mm, sample attached with conductive carbon tape); quantification technique, Linemarker PB-ZAF (Bruker Esprit 2.1 Software)).

Fig. 2 The top loading kiln used for the synthesis (left), the sources of brass (top right), and the self-made terracotta crucibles (bottom right)



UV-visible diffuse reflectance spectrophotometry (fiber optic reflectance spectroscopy)

Fiber optic reflectance spectroscopy (FORS) analysis was performed with an Avantes (Apeldoorn, The Netherlands) AvaSpec-ULS2048XL-USB2 model spectrophotometer and an AvaLight-HAL-S-IND tungsten halogen light source; detector and light source were connected with fiber optic cables to an FCR-7UV200-2-1.5 × 100 probe. In this configuration, both the incident and detecting angles were 45° from the surface normal, in order not to include specular reflectance. The spectral range of the detector was 200–1160 nm; the overall operational range of the device (combination of lamp+detector) was 375–1100 nm. Depending on the features of the monochromator (slit width 50 μm, grating of UA type with 300 lines/mm) and of the detector (2048 pixels), the best spectrum resolution was 2.4 nm calculated as FWHM. Diffuse reflectance spectra of the samples were referenced against the WS-2 reference tile provided by Avantes and guaranteed to be reflective at 98% or more in the spectral range investigated. The investigated area on the sample had a 1-mm diameter. The probe was inserted into an aluminum block, in order to exclude external light and to hold firmly the probe in place. In all measurements, the distance between probe and sample was kept constant to 2 mm. To visualize the investigated area on the sample, the probe contained a USB endoscope inserted as well in the block. The instrumental parameters were as follows: 10-ms integration time and 100 scans for a total acquisition time of 1.0 s for each spectrum. The whole system was managed by means of AvaSoft v. 8 dedicated software, running under Windows 7™.

X-ray powder diffraction

For the X-ray powder diffraction (XRPD) analyses, a SIEMENS D5000 X-ray powder diffractometer was used with Bragg Brentano geometry (Cu K α radiation, $\lambda = 1.54056 \text{ \AA}$; Department of Earth Sciences, University of Torino). The single-crystal data were collected with a Gemini R Ultra diffractometer with graphite-monochromated Mo-K α radiation ($\lambda = 0.71073 \text{ \AA}$) for cuprorivaite sample (synthesis ZA4) by the ω -scan method. The cell parameters were retrieved with the software CrysAlis PRO 1.171.38.46 (Rigaku 2015), and the same program was used to perform data reduction with corrections for Lorentz and polarizing effects. Scaling and absorption corrections were applied through the CrysAlisPro multiscan technique. The structure has been solved with the direct methods by using SHELXS-97 (Sheldrick 2008). All the structure has been refined with full-matrix least squares techniques on F2 with SHELXL-97. All non-hydrogen atoms were refined anisotropically. The possible replacement of Cu with Zn in the site of Cu has been tested, but no definable percentage has been found. The graphics of the crystal structure has been generated using Vesta (Momma and Izumi 2011). CCDC codes 1882695 contain the supplementary crystallographic data for cuprorivaite. These data can be obtained free of charge via <http://www.ccdc.cam.ac.uk/conts/retrieving.html> or from the Cambridge Crystallographic Data Centre, 12 Union Road, Cambridge CB2 1EZ, UK; fax: (+44) 1223-336-033 or e-mail: deposit@ccdc.cam.ac.uk.

Visible-induced luminescence

Visible-induced luminescence (VIL) was used for a preliminary characterization of EB formed in the syntheses (Dyer

et al. 2013). The images acquired were taken using a digital camera EOS 400D from which the IR filter had been removed. The sensitivity of the camera is up to 1000 nm. VIL images were produced using a B+W IR (093) BW72487 filter which allows the passage of not more than 1% of the radiation at 800 nm up to 88% at 900 nm. A LED lamp (YONGNUO YN300) with a very low emission in the infrared (IR) range was used as light source. It is important to note that the small amount of IR light emitted by the lamp can be used in this specific kind of VIL technique to give an enriched information: in black are visible IR absorbing materials and in gray are shown reflecting materials while the emitting materials (e.g., cuprorivaite) glow in white.

Results

Artificial sample production

Zn-enriched EB syntheses using brass as the source of copper have been performed in order to understand the structure and properties of the final product and correlate them to those of the conventional EB produced via salt-flux and solid-state syntheses. The samples have then been analyzed by means of FORS to describe their color and photoluminescence then by means of optical microscopy, SEM-EDS, and XRPD to describe the inner structures.

First of all, two preliminary experiments were performed to assess the best operative parameters to be used in the synthesis. The type A object has a content of zinc of about 42.4%. Such a concentration is typically obtainable with a speltering process, a technology developed later and commonly available in Europe only since the nineteenth century. The concentrations of zinc in the type B and type C objects were of about 22.2% and 17.6%, respectively, and are similar to the ones typically obtainable with the cementation production process (Bourgarit and Bauchau 2010; Craddock et al. 1990) even in the Middle Ages. Concentrations of iron in the range 0.7–0.9% were detected in all the brass investigated while lead was detected in an amount of 0.9–2.4% in the three objects, being type B the richer in this element. The three objects were part of furniture produced in Europe during the eighteenth–nineteenth centuries. After a surface cleaning, the samples were collected with tools (files and drill) that can produce particles analogous to the ones obtainable in the Middle Ages.

The brass powders were used to prepare different samples of Zn-enriched EB and to compare them with regular EB samples obtained via salt-flux and solid-state syntheses. It is noteworthy that we chose to use SiO₂ and CaCO₃ of commercial grade because their impurities could match quite well with the one expected for ancient productions (Pradell et al. 2006), as determined with SEM-EDS.

Table 1 Reactants used in preliminary experiments

Sample	SiO ₂ (g)	CaCO ₃ (g)	Cu source	Na ₂ CO ₃ (g)
SA1	0.38	0.16	0.10 g brass type A	0.06
SA2	0.28	0.12	0.10 g brass type A	0.06
SA3	0.42	0.18	0.10 g brass type A	0.06
SB1	0.38	0.16	0.10 g brass type B	0.06
SB2	0.28	0.12	0.10 g brass type B	0.06
SB3	0.42	0.18	0.10 g brass type B	0.06
SC1	0.38	0.16	0.10 g brass type C	0.06
SC2	0.28	0.12	0.10 g brass type C	0.06
SC3	0.42	0.18	0.10 g brass type C	0.06

The weights of reactants used in the preliminary experiments are shown in Table 1. In each synthesis, the respective reactants were finely ground and mixed in a ceramic mortar then put in porcelain crucibles and heated. The flux (Na₂CO₃) was added only in this series of experiments.

In the first preliminary experiment, samples of powders of brass of types A, B, and C were used for syntheses analogous to the traditional salt-flux method described by Vitruvius with the only variation of using brass instead of copper metal (Vitruvius 1999). As suggested in literature (Johnson-McDaniel and Salguero 2014; Mazzocchin et al. 2004; Riederer 1997; Warner 2011), SiO₂ and CaCO₃ were added in 4:1 stoichiometric ratio instead of sand. Na₂CO₃ about 10% w/w was added as a flux in place of natron. The mixtures obtained were initially heated with a rate of 2 °C/min until 875 °C and then held at 875 °C for 12 h. At the end, the temperature was cooled down to 20 °C with a cooling rate of 2 °C/min.

In the second experiment, similar mixtures of brass, SiO₂, and CaCO₃ were heated in the same way, but no flux was added and the temperature was raised to 975 °C. The conditions chosen for the second experiment are similar to those proposed in literature for the solid-state synthesis (Johnson-McDaniel and Salguero 2014). Once at room temperature, the crucibles of both preliminary experiments were photographed with the VIL technique to detect the presence of cuprorivaite-like materials formed.

Once determined that the 975 °C synthesis was the most effective in producing cuprorivaite-like materials from brass, some samples were prepared and refined. For this purpose, each of the 9 mixtures of reactants shown in Table 2 was finely ground in a ceramic mortar and put in a terracotta crucible. Then, they were heated with parameters analogous to the ones used in the second preliminary experiment. It may be worth remarking the fact that with the exception of the sample ZO, no fluxes were added in any mixture.

Once at room temperature and after VIL photography, solidified masses were removed by the crucibles and were crushed. Later, as suggested in literature, the samples were

Table 2 Reactants used in the main synthesis. The column on the left shows arbitrary names given to the mixtures. In the column on the right end, there are some notes on the stoichiometry ratios of elements in comparison with the ones of pure cuprorivaite

Sample	SiO ₂ (g)	CaCO ₃ (g)	Cu source	Na ₂ CO ₃	Comments
ZA	3.19	1.33	1.07 g brass type B	–	Excess Zn
ZB	3.19	1.03	1.37 g brass type B	–	Excess Zn and Cu, low Ca
ZC	3.19	1.11	1.29 g brass type C	–	Excess Zn and Cu, low Ca
ZM	3.19	1.33	0.85 g brass type A	–	Zn instead of Cu in cuprorivaite
ZN	3.19	1.33	0.85 g brass type B	–	Zn instead of Cu in cuprorivaite
ZO	3.19	1.33	0.85 g brass type B	0.10 g	Zn instead of Cu in cuprorivaite
ZP	3.19	0.96	1.08 g brass type B	–	Zn instead of Ca in cuprorivaite
ZR	3.19	1.33	0.84 g Cu	–	Cu metal standard
ZE	3.19	1.33	1.05 g CuO	–	CuO standard

washed to remove badly reacted material (Johnson-McDaniel and Salguero 2014; Warner 2011), soaking them in 50 ml of HCl 1 M for 48 h. Afterward, each powder was washed with 50 cc of distilled water and was filtered and dried. Three analogous cycles of reheating and crushing were then performed in order to improve the quality of the final products (Johnson-McDaniel and Salguero 2014; Riederer 1997; Warner 2011). However, other two samples were also used as references. The first was EB produced via the salt-flux synthesis analogous to the one used in the first preliminary experiment using CuO as the source of copper, washed in HCl for 48 h, and reheated and crushed other 3 times. To refer to this sample, the tag R4 was used. The second (referred as KR) was commercial EB purchased from Kremer Pigmente.

VIL imaging was used to visually identify any cuprorivaite produced (i.e., cuprorivaite glow in white). Results are shown in Fig. 3. From the results, it seems that the parameters commonly used in the standard salt-flux synthesis are not well suitable to produce EB from brass. Indeed, white luminescing areas are only clearly visible in the second experiment (Fig. 3b) that was carried out at 975 °C, i.e., at a temperature higher than the one commonly used for the standard salt-flux synthesis and at which the solid-state synthesis of cuprorivaite can occur (Delamare 1997; Etcheverry et al. 2001; Johnson-McDaniel and Salguero 2014).

The increase of luminescence going down in the rows of samples in Fig. 3b suggests that modern brass richer in zinc (SA series) is less suitable to produce EB than ancient brass with a lower zinc content (SB and SC series). The maximum of brightness seems however to be associated with the standard produced using straight copper metal. It seems that there are no appreciable differences among samples in the same row. A more comprehensive discussion of compositional features and a more detailed analytical characterization are further discussed above using refined samples produced in the main syntheses.

The artificial samples listed in Table 2 were produced in the main syntheses. By an optical inspection, we observe that after the first cycle of heating at 975 °C, all the samples with the

exception of ZE and ZR were blackish and cast in solid hard masses that copy the shape of the bottom of terracotta crucibles in the form of little shrunk blocks (see Fig. 4 left). To crush the blocks, a mortar was needed. An analogous behavior was observed in the production of R4 (i.e., using salt-flux synthesis) after the first cycle at 875 °C. ZE and ZR samples were instead observed as grayish soft solid friable material that can be crushed simply using a spatula (see Fig. 4 right).

After washing in HCl and the second cycle of reheating and crushing, all samples got markedly blue with different shades and deepness of hue, improving further their tone in the next two cycles. After each annealing, all the powdered samples changed again to hard blocks with the exception of ZE and ZR samples. ZA4 and ZN4 are the deepest blue color obtained and are quite similar in color to the salt-flux synthesis standards R4 and to the commercial one KR (see Fig. 5), while ZR and ZE where the lighter blue obtained.

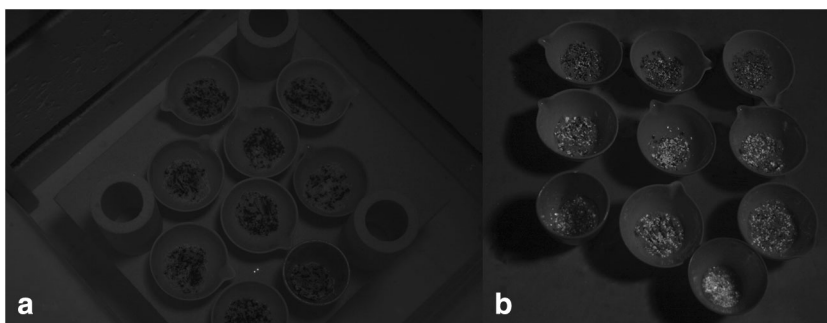
Since the end of the first cycle, all the samples produced showed some brightness in VIL images being ZR, ZE, ZA, and ZN the brightest and ZM one of the least bright. ZE was indeed brighter even than commercial Egyptian blue KR and a lot more than R4. A more accurate evaluation of luminescence and colors will be discussed in the next paragraph using FORS spectra.

Color and photoluminescence of the samples

As it is shown in Fig. 6a, the two main Zn-enriched EB produced (ZA4 and ZN4) have hue and intensity of reflectance that are very similar to the ones owed by the commercial EB purchased from Kremer Pigmente (KR). They have also a similar NIR reflectance and photoluminescence.

The most interesting data is however the outstanding behavior of cuprorivaite produced via solid-state synthesis ZE4 that shows a reflectance much higher than any other sample and a NIR total output (reflectance plus photoluminescence) higher than 95% in correspondence of the peak of VIL emission. Also ZR4, the other sample produced via the solid-state synthesis has a high NIR reflectance output if compared with the low

Fig. 3 VIL image of first (a) and second (b) preliminary experiment performed at 875 °C (a) and 975 °C (b). In both experiments, a standard was added. In the first preliminary experiment, two grains of R4 standard, and in the second, an internal standard produced using copper instead of brass (0.38 g SiO₂, 0.16 g CaCO₃, and 0.10 g Cu)



reflectance in the blue region. This is likely due, again, to the absence of any glassy phase on the surface of cuprorivaite crystals formed via the solid-state synthesis. The blue tone of ZE4 and ZR4 is definitely lighter than that of samples produced via the salt-flux synthesis. It is well known that a decrease in grain size can impart a lighter tone to EB (Delamare 1997; Riederer 1997; Warner 2011). Even if a smaller grain size is indeed observable (see Fig. 7 and Fig. 9), in particles produced via the solid-state synthesis, the effect may likely be increased by the higher scattering of light due to the lack of the quenching effect imparted by a glassy matrix. The comparison among the two samples produced via the solid-state synthesis (ZE4 and ZR4) indicates a great difference between them probably due to the fact that in ZR4 there is a widespread presence of unreacted copper metal grains (see Fig. 7 and Fig. 9b) that somehow could be responsible for the decrease in reflectance (Fig. 6a). The low degree of reaction is probably the cause of the shift in color to green likely due to the presence of CuO and/or metal particles and other Cu-containing silicates. This indicates that unless copper metal particles are very thin, CuO is more effective than copper metal as a reactant to produce cuprorivaite via the solid-state synthesis. This is consistent with what was concluded by Pradell et al. (2006) suggesting that in antiquity, a method such the one described by Vitruvius (i.e., using copper filings) but without the use of natron was difficult to perform because if it turns in a solid-state synthesis, the final product is of very poor quality (i.e., too pale color and a lot of unreacted material).

A further consideration can be made regarding the salt-flux synthesis standard (sample R4). Even if it shows a very

intense deep-blue hue, it has indeed a quite weak NIR photoluminescence likely due to the presence of a high amount of glass around the particles (see Fig. 9a).

In Fig. 6b, a comparison is shown between the samples of Zn-enriched EB produced. In general, if we exclude ZA4 and in a minor extent ZN4, all other samples show a slight shift to green in comparison with KR and with Egyptian blue produced via the standard salt-flux and solid-state synthesis. The reason can be an unbalance in calcium vs copper molar concentration. A higher value of calcium can indeed impart a green shade (Hatton et al. 2008; Pagès-Camagna et al. 1999; Riederer 1997). This behavior can explain the results obtained for ZM4 and ZO4 that indeed are the greenest samples of this group. In these two cases, the presence of a very high amount of Zn in sample ZM4 (and a very low Cu) or the presence of some Na from the flux in the sample ZO4 that can somehow compete with Ca can explain the greater green shift of these two samples in comparison with ZN4. The other samples are characterized by excess of both Cu and Zn that likely can account for the formation of silicates and glasses that can have a green or turquoise hue. Micro photographs of some samples produced are shown in Fig. 7.

The sample ZA4 produced with brass and without any added flux looks very similar to the sample of pigment KR, supporting the notion that such a pigment can be indeed analogous to the one used in Castelseprio where a substitute of conventional EB was likely used. However, also ZN4 and the salt-flux standard sample R4 (not shown in Fig. 7) have a very similar aspect, with some sporadic green particles only observable in ZN4. ZM4 has instead a significant number of

Fig. 4 Image of ZP (left) and ZE (right) sample after the first cycle of heating at 975 °C

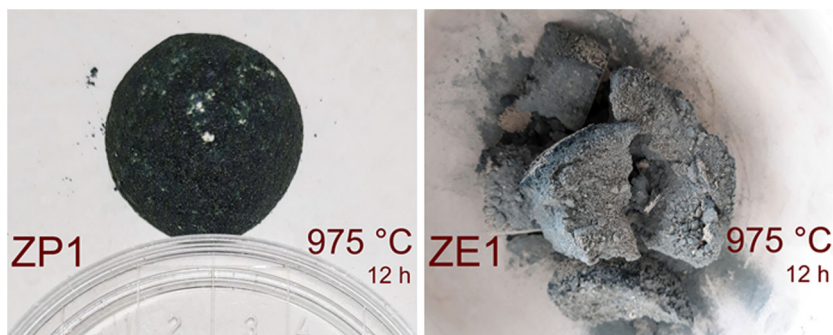
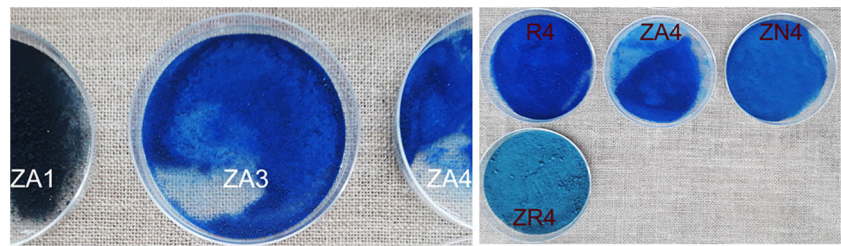


Fig. 5 Images of samples obtained in the main syntheses



green particles. The XRPD data reported in Fig. 8 clearly show that the only appreciable difference between the samples ZA4 and ZM4 is a relevant amount of silica that is present only in ZM4. It is very likely that analogously to what happens in Egyptian green, a green glassy phase can locally trap Cu^{2+} ions and silica (Hatton et al. 2008; Pagès-Camagna and Colinart 2003), both likely formed due to the unbalance in the Ca/Cu and by the high amount of Zn present. This result is also consistent with the observation made in the preliminary experiment (Fig. 3) showing that modern brass now commonly available seem to be a very poor choice for the production of Zn-enriched EB. Also samples ZO, ZP, and ZC show such a kind of green particles even if in a minor amount in respect to ZM4.

The micrographs in Fig. 7 show also clearly that samples ZE4 and ZR4 produced via the solid-state synthesis have a lighter shade and thinner particles than any other sample. Unreacted metal copper particles are clearly visible in the sample ZR4, where also green particles are observable. This is likely due to the unbalance in the reaction that was determined by the temporary unavailability of the copper fixed in the bulk of the metal particles.

Synthetic routes and microstructure

Samples of powder embedded in polyester and lapped were observed and analyzed with SEM-EDS to show structure, shape, and nature of the particles produced during the synthesis and to better understand the process involved. In the first image (Fig. 9), particles produced via the salt-flux synthesis (sample R4) and solid-state synthesis (sample ZE4) are compared.

The salt-flux synthesis of cuprorivaite is dominated by the process of nucleation and growth of the cuprorivaite crystals within a liquid or glass phase (Delamare 1997; Pradell et al. 2006). If we observe and analyze with EDS some grains of sample R4 (Fig. 9a), we can indeed clearly recognize large crystals of pure cuprorivaite with a peculiar elongated rectangular shape that are surrounded by a glassy matrix. Cuprorivaite crystals in such an environment grow around a nucleus of crystallization that is often a grain of silica (Delamare 1997). In the solid-state synthesis, instead, the only process involved is that of surface diffusion of ions of the three components (Delamare 1997; Pradell et al. 2006). They generally take place into the surface of a grain of silica (Delamare 1997). Such phenomena can be clearly seen in Fig. 9b where some grains of ZR4 are shown. In particular, a big grain of unreacted copper in contact with a silica grain shows perfectly the growing cuprorivaite on the

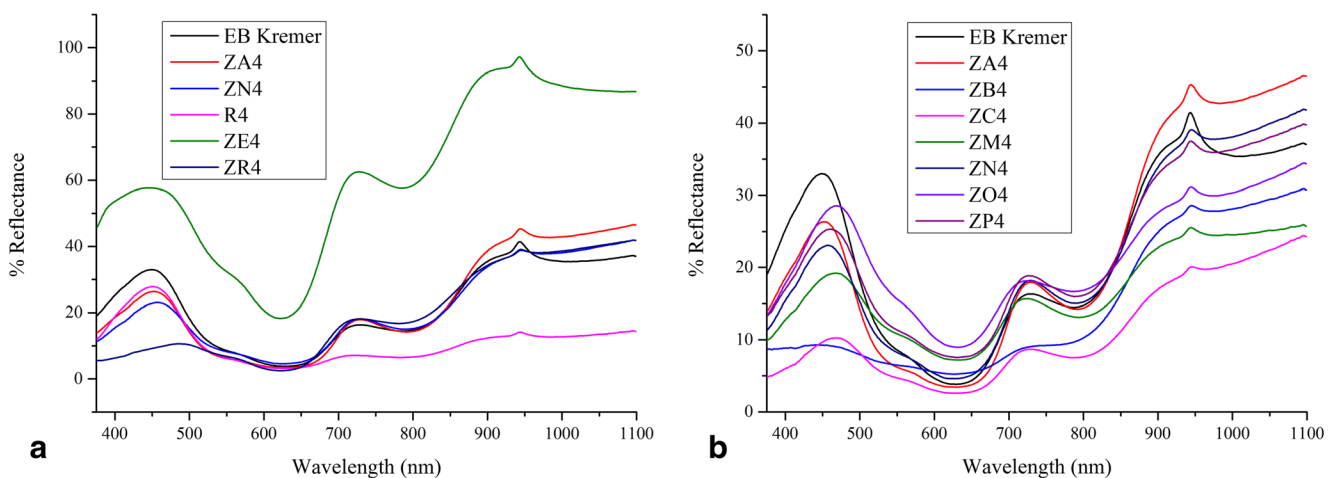
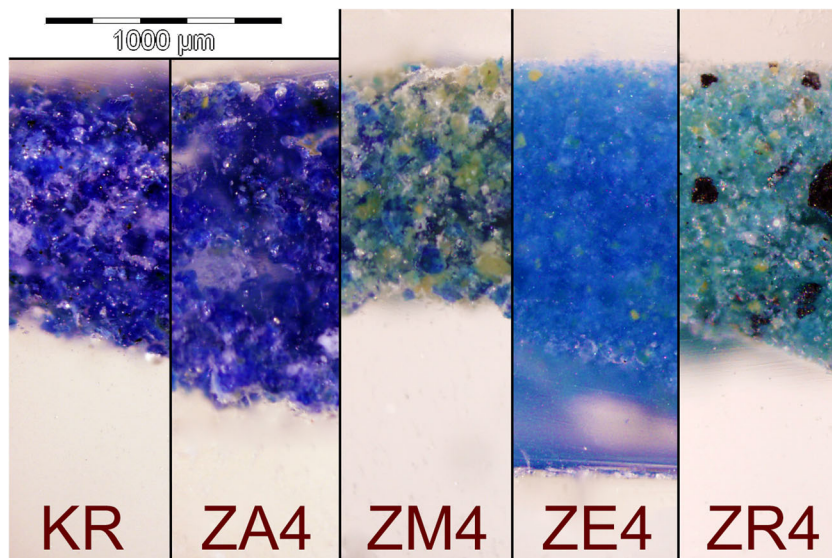


Fig. 6 **a** FORS spectra of standard EB produced via salt-flux synthesis and solid-state synthesis compared with spectra of samples of Zn-enriched EB produced from brass. **b** Comparison of FORS spectra of samples of Zn-enriched EB produced with stoichiometric and non-stoichiometric component

Fig. 7 Images acquired through optical microscopy on samples KR, ZA4, ZM4, ZE4, and ZR4 after the embedding of the powder particles in polyester resin and lapping



surface of contact; arrows in the figure indicate reaction interfaces. Cuprorivaite is also present on the surface of

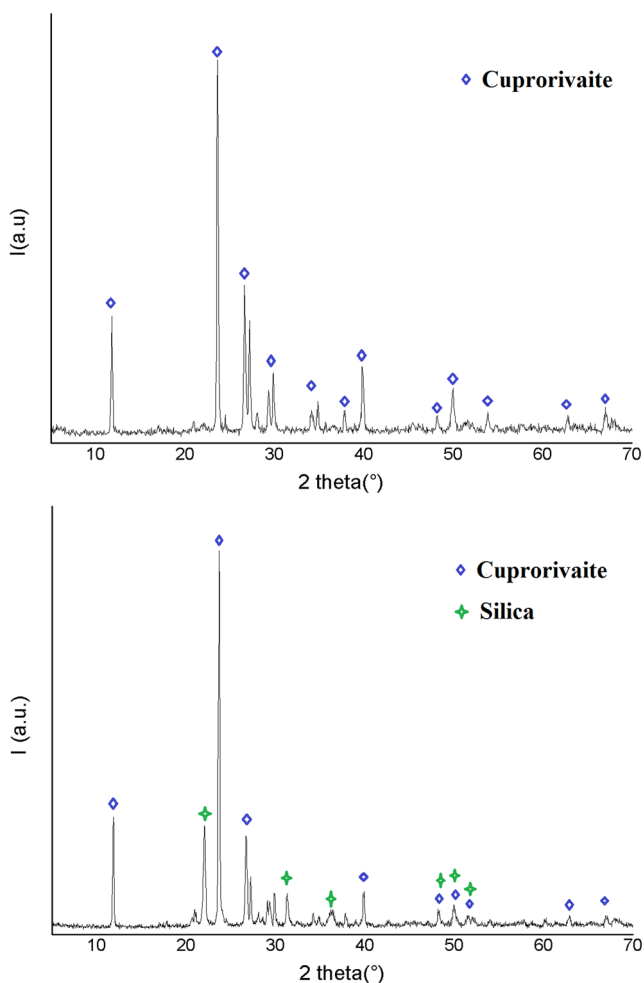


Fig. 8 XRPD diffractograms of samples ZA4 (right) and ZM4 (left)

any silica grain, recognizable in the photo as a thin lighter layer surrounding the silica particles. It is important to note the lack of a substantial glassy phase and the direct contact of the cuprorivaite formed with the surrounding environment. Such grains are undoubtedly smaller than the ones formed by the salt-flux synthesis. They retain about the same size of silica grains (Delamare 1997).

Observing the sample ZA (produced with brass and no added fluxes) after the first cycle of heating (Fig. 10a), it is clearly recognizable the same structure of cuprorivaite formed via the salt-flux synthesis.

As shown in EDS spectra reported in Fig. 10, crystals of pure cuprorivaite are surrounded by a matrix rich in zinc. The nature of the matrix is likely a glass, being however not observable any zinc mineral in XRPD data (see Fig. 8). It is important to note the presence of a small amount of aluminum and potassium registered generally in EDS spectra of the glassy matrix. These elements present in the starting reactants as trace elements can also derive from potassium aluminum silicates in the terracotta crucibles surface such as orthoclase. Zinc is a secondary flux whose fluxing action starts at around 1000 °C (Casasola et al. 2012; Moezzi et al. 2012), i.e., at a temperature analogous to the one used for the synthesis. At this temperature, it can interact with the potassium aluminum silicate and form a glassy phase (Casasola et al. 2012). Minor amounts of lead are also observable in the matrix. They come from the small amount of Pb commonly present both in modern and ancient brass and contained in the range 0.9–2.4% in the brass used. Also, lead can act as a flux and can further promote the formation of a glassy matrix (Casasola et al. 2012). A weak peak at 6.4 keV is also observable in the glass matrix and can be related to the iron present in the starting brass samples.

Fig. 9 SEM-EDS images showing particles produced via (A) salt-flux synthesis and (B) solid-state synthesis

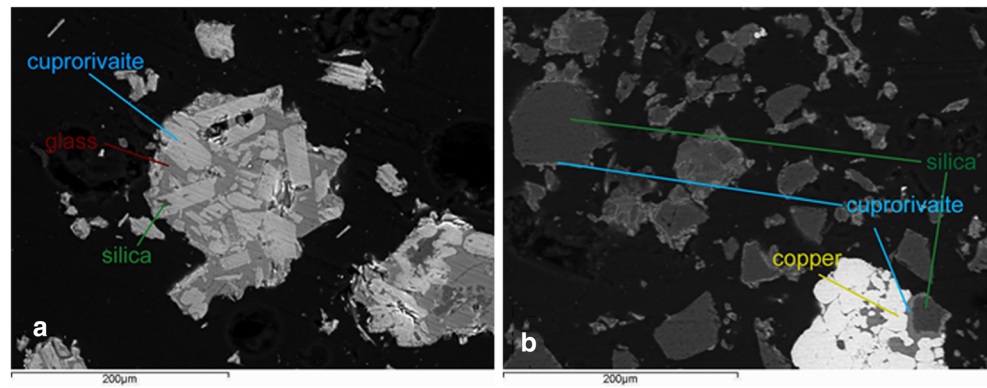


Figure 10b shows some grains of ZA4 that are obtained after washing ZA1 and having 3 more cycles of reheating and crushing. Figure 11a and b show similar results on ZN4 sample. In salt-flux-synthesized samples, each reheating phase is indeed an annealing in which crushed grains can be sintered (Delamare 1997) as macroscopically observed also by the formation of solid casts at the end of each cycle. As a consequence of annealing, the glassy residual phase can fill narrow spaces (Fig. 10b), the cuprorivaite crystals can grow further (Fig. 11b), and other minerals can be formed as can be observed in the upper lighter part of the grain in Fig. 11a where a Zn–Ca silicate compound can be identified via SEM-EDS and can be argued to be clinohedrite. To further demonstrate the

absence of any Zn substitution in the crystalline cuprorivaite, the crystal structure has been re-determined via XRD from a single crystal obtained by ZA4 synthesis (see supporting information), and no proof of this phenomenon has been found with respect to the crystal structure of literature (Chakoumakos et al. 1993).

Comparison with ancient Zn-rich Egyptian blue sample

This section compares the sample of ancient blue pigment from Castelseprio (CS) with the previous results presented

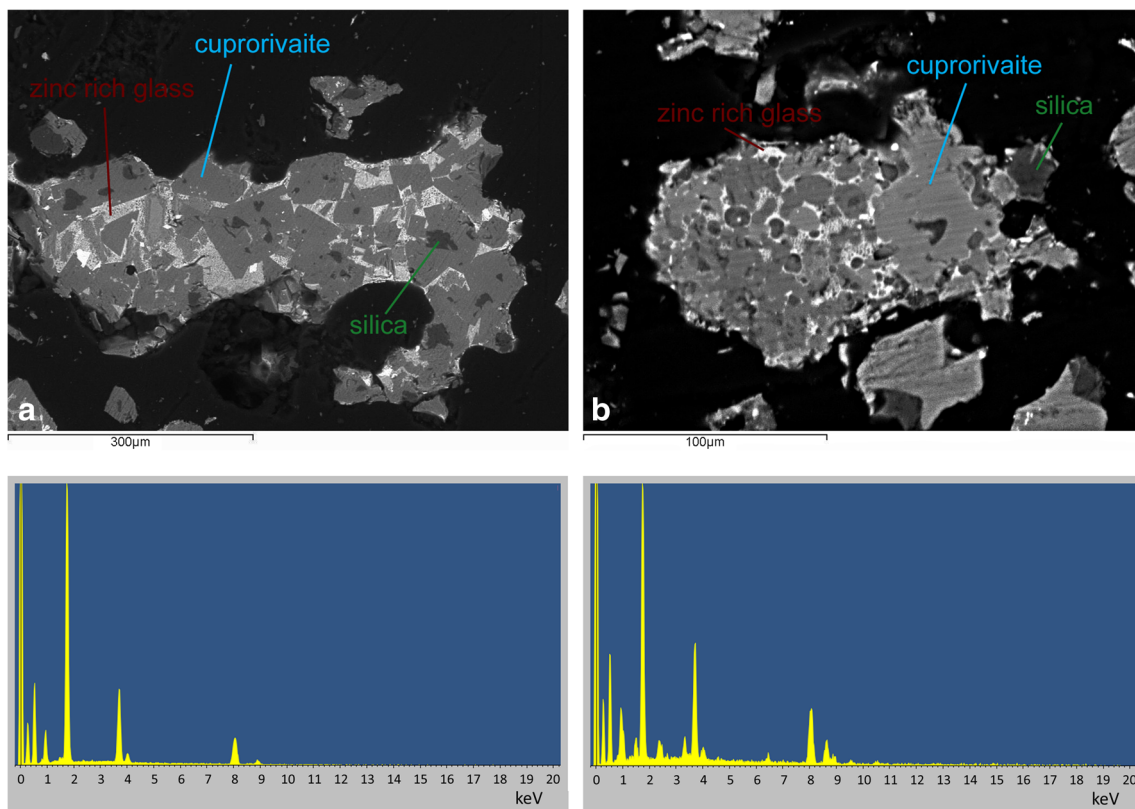
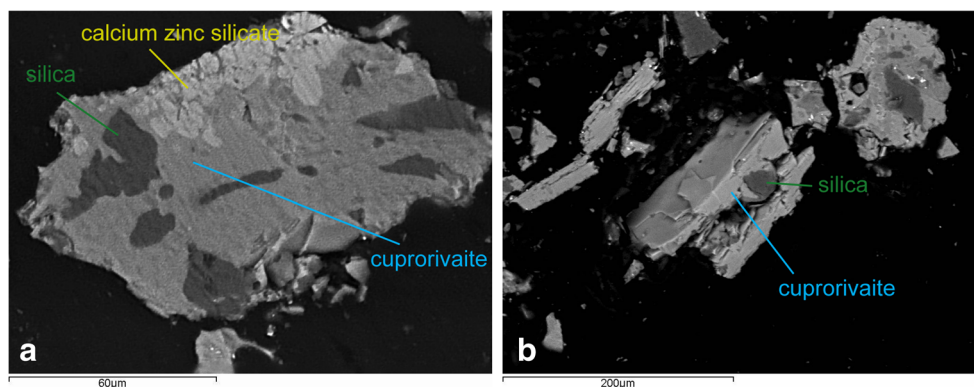


Fig. 10 Top: SEM-EDS images showing ZA sample particles produced **a** after the first cycle of heating and **b** after the fourth cycle of heating. Bottom: corresponding EDS spectra of cuprorivaite (left) and zinc-rich glass (right)

Fig. 11 SEM-EDS images showing ZN4 sample particles



on modern replicas. Figure 12 highlights the results from optical microscopy and SEM-EDS.

The particles of the ancient pigment reach a maximum size of about 40 µm. Figure 12a clearly shows the presence of blue pigment in the sample. In the BSE image (Fig. 12b), the grain of EB is selected for further analysis. In the BSE image of the grain (Fig. 12c), an inner structure is recognizable. It includes darker, almost rectangular zones of cuprorivaite (Fig. 12d) surrounded by a lighter matrix rich in zinc (Fig. 12f). By mapping the elemental composition across the ancient grain (Fig. 12d), the gradation of the copper-rich cuprorivaite phase into the zinc-rich glass phase is seen. Pockets of the copper-rich phase are seen surrounded by the zinc-rich glass. Even if the dimensions of the cuprorivaite crystals seems to be smaller and the border seems to be less narrow, the structure is consistent with the one observed for artificial samples of Zn-enriched EB (e.g., Fig. 12g, h). In comparison, the EDS map of the modern reproduction, ZA1 (Fig. 12h), shows similar gradation between copper-rich and zinc-rich phases; however, instead of pockets of the copper-rich phase within the zinc-rich glass, we instead see clasts of the zinc-rich phase forming.

The elemental distribution confirms that a heterogeneous interleaving of phases is favored over a homogenous incorporation of zinc into the EB. The differences probably depend on some parameters such as a thinner grinding of the pigment between the cycles of reheating or differences in time of heating and cooling. However, the data demonstrate that the production method proposed is a viable route to obtain an analogous, newly produced Zn-enriched EB pigment, very close to the ancient one present in Castelseprio Early Medieval mural paintings.

Discussion

Zn-enriched EB syntheses using brass as the source of copper were performed in order to understand the structure and properties of the final product and correlate them to those of the conventional EB produced via the salt-flux and solid-state syntheses. Apart from the general interest in trying to

understand the ancient technology used, a better understanding in structure, properties, and process of formation of cuprorivaite crystals could contribute to enlarge the family of NIR photoluminescent materials. Zn-enriched EB produced resulted similar to the one used in Castelseprio during the Early Middle Ages whose production technology is lost (Nicola et al. 2018a).

Archeology-inspired Zn-enriched EB production was never reported before. In a series of samples artificially produced from brass and from standard copper (both copper metal and copper oxide), color and intensity of photoluminescence have been put in relationship with composition, mechanism of formation, and inner structure. At this purpose, different syntheses have been performed to evaluate the effect of parameters like the nature of the main constituents, their concentration, temperature, and time of heating. After a detailed description of sample production done also with the help of the VIL imaging technique, FORS spectra have been used to describe color and photoluminescence of the samples produced while optical microscopy, SEM-EDS, and XRPD have been used to describe the inner structures.

The observed unsuitability of modern standard brass type A that contains 42% of Zn for the production of Zn-enriched EB is consistent with Li et al. (2014), which stated that a concentration of Zn higher than 30% is above the solid solubility of Zn^{2+} in the cuprorivaite. However, our results on samples in which by concentration and stoichiometry Zn^{2+} could have substituted Cu^{2+} indicate that a possible zinc-doped cuprorivaite having a formula $CaCu_{1-x}Zn_xSi_4O_{10}$, where x is in the order of 0.1 or higher, seems not to form.

Similarly in any of the syntheses tested with SEM-EDS, it is not possible to observe any crystal of $Ca_{1-x}Zn_xCuSi_4O_{10}$, even when there was a lack of Ca^{2+} in the reactants that could be replaceable by Zn^{2+} (Salguero et al. 2014). Thus, we can argue that the existence of a significant zinc substituted cuprorivaite has still to be confirmed.

In all the samples prepared from brass, a structure was observed that is very close to the one of conventional EB produced via the salt-flux synthesis. It was observed even if neither Na^+ nor K^+ bearing flux was added at all. The zinc was

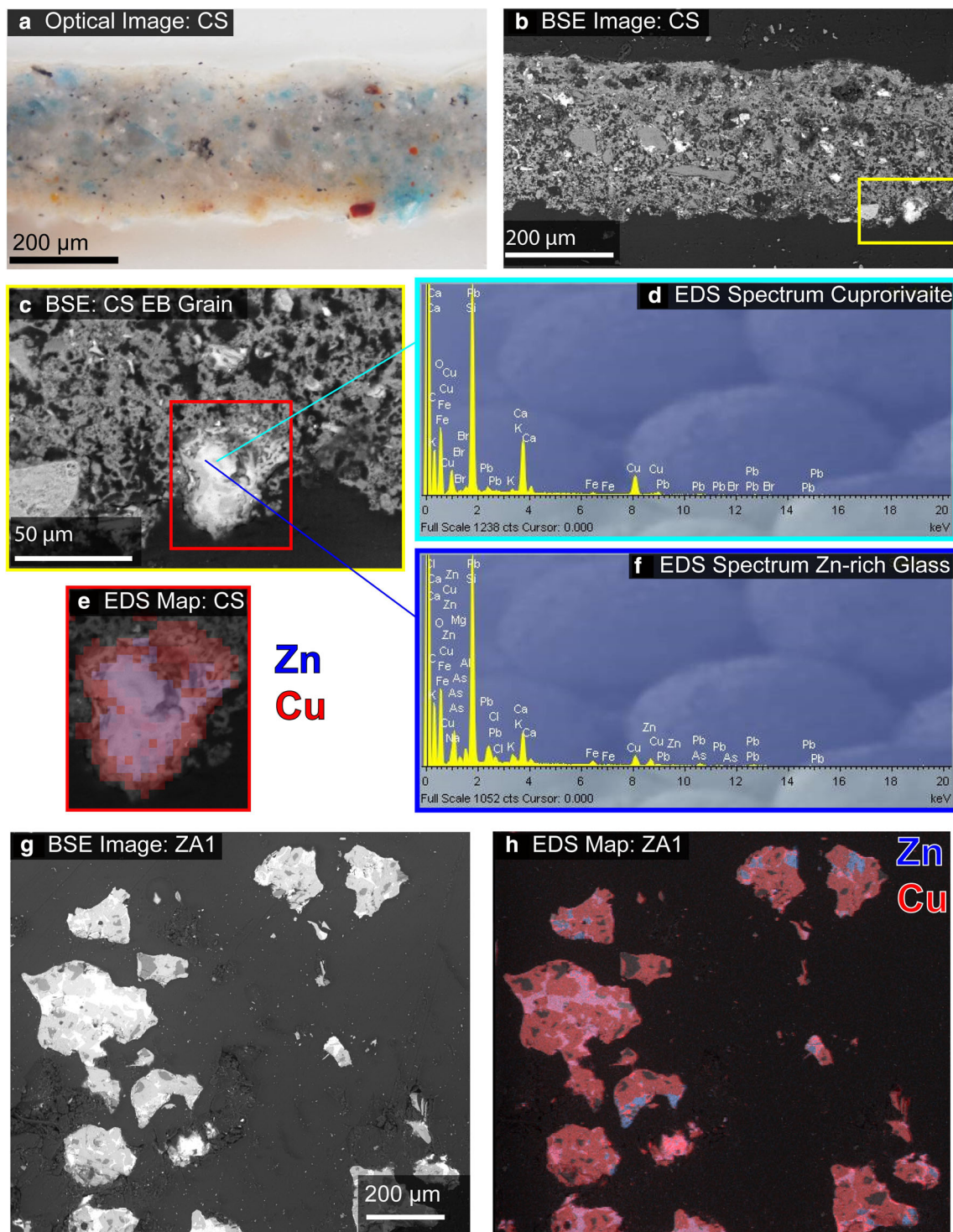


Fig. 12 **a** Optical image of the ancient CS sample. **b** BSE image of the same area showing the position of the EB grain. **c** BSE image of the ancient EB grain. **d** EDS spectrum of cuprorivaite in the EB grain. **e** EDS map of the EB grain showing Zn and Cu distribution. **f** EDS

spectrum of the Zn-rich glassy phase in the ancient EB grain. **g** BSE image of modern reproduction sample ZA1. **h** EDS map of sample ZA1 showing distribution of Zn and Cu

in general present in all the glassy matrices formed, and sometimes it crystallizes in other minerals or seems to hide in very narrow cracks and structures in annealed specimens. It has to be noted that Zn itself can act as a secondary flux starting to

work at temperature close to 1000 °C (Moezzi et al. 2012), and that likely it can improve the effect of small amount of fluxes contained in the reactants or maybe even stripped from the crucible walls (e.g., orthoclase) if it is made in terracotta or

ceramic materials. This fact could have permitted to produce EB in the Middle Ages even if the very rare and expensive flux natron was not available. Indeed, during the seventh–ninth centuries, a general crisis in the supply of natron happened (Shortland et al. 2006), which is almost at the same time when the Castelseprio frescoes were painted (Nicola et al. 2018a). We can, therefore, formulate the hypothesis that the development of this kind of production of EB requiring higher temperatures but no addition of fluxes could have been a response to a lack of natron supply. The need to shift from a well-known flux (natron) to other kind of fluxes (i.e., plant ashes) that maybe were used in the far past but are probably widely forgotten and lost implies a research step and to modify ancient recipes. While this seems to have happened for glassmaking during the seventh–ninth centuries (Shortland et al. 2006), for some reasons, it seems that a similar technological evolution had not happened in EB production. Our hypothesis is that the development of Zn-rich EB production is a step in this technological struggle to go beyond conventional EB production with natron. Eventually, while the use of plant ash is the final answer to the crisis in glassmaking, a similar result was probably never reached for EB production. Its technology of production seemingly has been lost and forgotten during this period while Zn-enriched production only developed at local area (Byzantine area—probably Turkey) as a secret that in a certain moment got lost.

This may have been also favored by the increased availability of brass (Craddock et al. 1990) that started with the first centuries of the Common Era; however, we are not able to state whether ancient artisans used brass prepared at the purpose or reused previously prepared brass. This technique may have allowed to produce a deep-blue pigment analogous to the ancient “artificial lapis lazuli” EB without the use of the expensive natron. The advent of the very expensive blue pigment made by natural lapis lazuli seems to have eventually substituted EB (Gaetani et al. 2004). The reason why it happened is not fully understood, but the availability of Zn-enriched EB only at small scale and likely as a result of a well-kept secret recipe may have in the end caused a lack of knowledge that resulted in the loss of this technology. As a support for this hypothesis, it has to be pointed out that Zn-enriched EB was found only in Castelseprio (Nicola et al. 2018a) and St. Philip of Hierapolis (Vettori et al. 2019) that are both early medieval Byzantine culturally influenced productions. It may be expected that in the future, new findings of Zn-enriched Egyptian blue may occur in similar contexts.

We can however observe that the use of the experimental archeology approach has allowed obtaining interesting data that possibly would have not been observable using a more standard approach. The small contribution of primary fluxes from reactants and maybe from the crucible would have been indeed not observable using a more conventional approach.

From the point of view of the present and future applications of cuprorivaite as a NIR photoluminescent class of materials, we can observe that the results obtained in the present work add a viable route of synthesis for a new kind of Zn-enriched glass material. More in general, the results obtained on conventional and Zn-enriched EB suggest that with the aim of improving the quality and amount of NIR emission and reflection, a key factor should be the internal structure and process of synthesis employed. Indeed, the presence of glassy matrix around the crystals of cuprorivaite can decrease dramatically the efficiency as IR photoluminescent emitter and overall NIR reflecting material also because copper-containing glassy phases like amorphous $\text{Na}_2\text{CuSi}_4\text{O}_{10}$ (Kawamura and Kawahara 1977), whose presence in EB was suggested by Onoratini et al. (1987), can be strong IR absorbers. On the other hand, the lack of glassy phase around solid-state-produced crystals can improve drastically their IR reflectance (much more than in the visible region) and if well managed can help to produce better NIR photoluminescent materials.

Conclusions

In this work, apart the salt-flux and solid-state syntheses of standard EB, a new route of synthesis of Zn-enriched EB pigments is presented. The possibility to produce Zn-enriched EB from brass was inspired by the recently uncovered zinc-bearing EB found on the early medieval mural paintings of Santa Maria *foris portas* Church at Castelseprio. Both ancient samples and modern replicas were analyzed in order to pinpoint the zinc environment inside the pigment microstructure. Zn was found to be concentrated in a glass-based matrix surrounding cuprorivaite crystals, indicating that a possible zinc-doped cuprorivaite of the formula $\text{CaCu}_{1-x}\text{Zn}_x\text{Si}_4\text{O}_{10}$, (where x is in the order of 0.1 or higher) seems not to form at indicated conditions of synthesis. The relationship between the microstructure and the NIR photoluminescence of this important class of pigments was investigated with the objective of verifying whether the use of such a non-traditional source for synthesis of EB had been intentional or not. The results of the investigation apparently point to an intentional, highly skillful technology. Considering the actual scarceness of diagnostic evidences of Zn-enriched EB, further investigation is needed to verify where this technology comes from and whether—or not—it was typical of one geographic source, one culture, or one period only.

Besides this, it is interesting to explore how an ancient technology could be exploited for possible modern applications. Variations of EB prepared through the solid-state

synthesis resulted in a pigment with particularly efficient NIR photoluminescence emission and VIS-NIR reflectance, compared with the standard EB salt-flux synthesis.

Acknowledgments We are thankful to the agencies of Soprintendenza in charge for Castelseprio for authorizing technical analyses in 2012. We thank Giacomo Chiari for his kind advice and cooperation. We are also grateful for the technical assistance of Vincenzo Gheroldi in historical contextualization, Alessandro Marello in SEM-EDS analyses, Nadia Curetti in XRPD analyses, Gian Luigi Nicola in the archeological approach definition, Gerardo Radogna for the supply of ancient brass, Nicola Pisano and Gianna Tognin for the help in some phases of production of Zn-enriched EB, and Giovanna Fazzone for statistical analysis and support.

Compliance with ethical standards

Conflict of interest The authors declare that they have no conflict of interest.

References

- Accorsi G, Verri G, Bolognesi M, Armaroli N, Clementi C, Miliani C, Romani A (2009) The exceptional near-infrared luminescence properties of cuprorivaite (Egyptian blue). *Chem Commun*:3392–3394
- Bensi P (1990) La pellicola pittorica nella pittura murale in Italia: materiali e tecniche esecutive dall'alto medioevo al XIX secolo. In: Danti C, Matteini M, Moles A (eds) *Le pitture murali. Tecniche, problemi, conservazione*. Centro Di, Firenze, pp 73–102
- Berdahl P, Boocock SK, Chan GCY, Chen SS, Levinson RM, Zalich MA (2018) High quantum yield of the Egyptian blue family of infrared phosphors (MCuSi₄O₁₀, M = Ca, Sr, Ba). *J Appl Phys* 123:193103
- Berke H (2007) The invention of blue and purple pigments in ancient times. *Chem Soc Rev* 36:15–30
- Bertoni A (2003) Il ciclo pittorico di Santa Maria foris portas. La scoperta, le correnti interpretative, le problematiche, i risultati. In: Limonta D, Bertoni A, De Marchi PM (eds) *Castelseprio e la Giudicaria. Cinquant'anni di studi: resoconti e nuove prospettive*, Milano Liceo artistico Frattini, Varese, pp 45–83
- Bertrand L, Gervais C, Masic A, Robbiola L (2018) Paleo-inspired systems: durability, sustainability, and remarkable properties. *Angew Chem Int Ed* 57:7288–7295
- Borisov SM, Würth C, Resch-Genger U, Klimant I (2013) New life of ancient pigments: application in high-performance optical sensing materials. *Anal Chem* 85:9371–9377
- Bourgarit D, Bauchau F (2010) The ancient brass cementation processes revisited by extensive experimental simulation. *Archaeotechnology* 62:27–33
- Bredal-Jørgensen J, Sanyova J, Rask V, Sargent ML, Therkildsen RH (2011) Striking presence of Egyptian blue identified in a painting by Giovanni Battista Benvenuto from 1524. *Anal Bioanal Chem* 401:1433–1439
- Broggiolo GP (2013) La stratigrafia muraria. In: De Marchi PM (ed) *Castelseprio e Torba: sintesi delle ricerche e aggiornamenti*. SAP Società Archeologica s.r.l., Mantova, pp 223–254
- Caponetti E, Francesco A, Chillura Martino D et al (2017) First discovery of orichalcum ingots from the remains of a 6th century BC shipwreck near Gela (Sicily) seabed. *Mediterr Archaeol Archaeom* 17:11–18
- Caley ER (1964) Orichalcum and related ancient alloys. *American Numismatic Society*, New York, p 151
- Casasola R, Rincón JM, Romero M (2012) Glass-ceramic glazes for ceramic tiles: a review. *J Mater Sci* 47:553–582
- Chakoumakos BC, Fernandez-Baca JA, Boatner LA (1993) Refinement of the structures of the layer silicates MCuSi₄O₁₀ (M = Ca, Sr, Ba) by Rietveld analysis of neutron powder diffraction data. *J Solid State Chem* 103:105–113
- Chaptal J (1809) Sur quelques couleurs trouvees a Pompeia. *Ann Chim* 70:22–31
- Chen Y, Kan M, Sun Q, Jena P (2016) Structure and properties of Egyptian blue monolayer family: XCuSi₄O₁₀ (X = Ca, Sr, and Ba). *J Phys Chem Lett* 7:399–405
- Chiari G (2018) Photoluminescence of Egyptian blue. In: López Varela S (ed) *The SAS Encyclopedia of Archaeological Sciences*. Wiley, New York. <https://doi.org/10.1002/9781119188230.saseas0453>
- Corcoran L (2016) The color blue as an animator in ancient Egyptian art. In: Goldman RB (ed) *Essays in global color history: interpreting the ancient spectrum*. Gorgias Press, Piscataway, pp 43–63
- Craddock PT, La Niece SC, Hook DR (1990) Brass in the medieval Islamic world. In: Craddock PT (ed) *2000 years of zinc and brass*, British museum occasional paper, vol 50. British Museum, London, pp 73–102
- Humphry D (1815) Some experiments and observations on the colours used in painting by the ancients. *Philos Trans R Soc Lond* 105:97–124
- Delamare F (1997) Sur les processus physiques intervenant lors de la synthèse du bleu égyptien: réflexion à propos de la composition de pigments bleus gallo-romains. *Rev d'Archéométrie* 21:103–119
- Dyer J, Verri G, Cupitt J (2013) Multispectral imaging in reflectance and photo-induced luminescence modes: a user manual A User Manual. European Charisma Project. <https://www.britishmuseum.org/pdf/charisma-multispectral-imaging-manual-2013.pdf>. Accessed 02 March 2019
- Errington B, Lawson G, Lewis SW, Smith GD (2016) Micronised Egyptian blue pigment: a novel near-infrared luminescent fingerprint dusting powder. *Dyes Pigments* 132:310–315
- Etcheverry MP, Schvoerer M, Bechtel F (2001) Bleu égyptien: mise en évidence de deux processus de formation de la cuprorivaite. *Rev d'Archéométrie* 25:87–100
- Fenoglio G, Agostino A, Aceto M, D'Amicone E, Vigna L (2012) I pigmenti blu e verdi degli Egizi. Nuove ricerche ed analisi al Museo Egizio di Torino. In: Riccardi MP, Basso E (eds) *Proceedings of AIAR10 Congress*. Patron Editore, Bologna
- Gaetani MC, Santamaria U, Seccaroni C (2004) The use of Egyptian blue and lapis lazuli in the Middle Ages: the wall paintings of the San Saba church in Rome. *Stud Conserv* 49:13–23
- García-Fernández P, Moreno M, Aramburu JA (2015) Origin of the exotic blue color of copper-containing historical pigments. *Inorg Chem* 54:192–199
- Gheroldi V (2013) I rivestimenti aniconici e i dipinti murali dell'abside est della chiesa di Santa Maria foris portas. In: De Marchi PM (ed) *Castelseprio e Torba: sintesi delle ricerche e aggiornamenti*. SAP Società Archeologica s.r.l., Mantova, pp 255–291
- Gheroldi V (2017) Sequenze e datazioni. Le finiture aniconiche e i dipinti murali dell'abside est di Santa Maria foris portas di Castelseprio. *Rivista della Società Storica Varesina XXXI*:1–25 (in press)
- Giménez J, Espriu-Gascon A, Bastos-Arrieta J, de Pablo J (2017) Effect of NaCl on the fabrication of the Egyptian blue pigment. *J Archaeol Sci Rep* 14:174–180
- El Goresy A, Schiegl S, Weiner KL (1996) A chronological scheme for the technological evolution of copper in ancient Egypt. In: Ismael FA (ed) *Proceedings of the First International Conference on Ancient Egyptian Mining & Metallurgy and Conservation of Metallic Artifacts*. Egyptian Antiquities Organization Press, Cairo, pp 215–234
- Greenwood NN, Earnshaw A (1997) *Chemistry of the elements*, 2nd edn. Elsevier, Amsterdam

- Hatton GD, Shortland AJ, Tite MS (2008) The production technology of Egyptian blue and green frits from second millennium BC Egypt and Mesopotamia. *J Archaeol Sci* 35:1591–1604
- Ingo GM, Çilingiroğlu A, Di Carlo G, Batmaz A, De Caro T, Riccucci C, Parisi EI, Faraldi F (2013) Egyptian blue cakes from the Ayanis fortress (Eastern Anatolia, Turkey): micro-chemical and -structural investigations for the identification of manufacturing process and provenance. *J Archaeol Sci* 40:4283–4290
- Jaksch H, Seipel W, Weiner KL, El Goresy A (1983) Egyptian blue—cuprorivaite a window to ancient Egyptian technology. *Naturwissenschaften* 70:525–535
- Johnson-McDaniel D, Barrett CA, Sharafi A, Salguero TT (2013) Nanoscience of an ancient pigment. *J Am Chem Soc* 135:1677–1679
- Johnson-McDaniel D, Salguero TT (2014) Exfoliation of Egyptian blue and Han blue, two alkali earth copper silicate-based pigments. *J Vis Exp* 86:e51686
- Kaczmarczyk A, Hedges REM (1983) Ancient Egyptian faience: an analytical survey of Egyptian faience from predynastic to Roman times. *Aris and Phillips, Warminster*
- Kakoulli I, Radpour R, Lin Y, Svoboda M, Fischer C (2017) Application of forensic photography for the detection and mapping of Egyptian blue and madder lake in Hellenistic polychrome terracottas based on their photophysical properties. *Dyes Pigments* 136:104–115
- Katsaros T, Liritzis I, Laskaris N (2010) Identification of Theophrastus' pigments *egyptios yanos* and *psimythion* from archaeological excavations. *ArchéoSciences* 34:69–80
- Kawamura K, Kawahara A (1977) The crystal structure of synthetic copper sodium silicate: $\text{CuNa}_2\text{Si}_4\text{O}_{10}$. *Acta Crystallogr B* 33:1071–1075
- Lazzarini L (1982) The discovery of Egyptian blue in a Roman fresco of the mediaeval period (ninth century). *Stud Conserv* 27:84–86
- Li YJ, Ye S, Wang CH, Wang XM, Zhang QY (2014) Temperature-dependent near-infrared emission of highly concentrated Cu^{2+} in $\text{CaCuSi}_4\text{O}_{10}$ phosphor. *J Mater Chem C* 2:10395–10402
- Lliveras A, Torrents A, Giráldez P, Vendrell-Saz M (2010) Evidence for the use of Egyptian blue in an 11th century mural altarpiece by SEM-EDS, FTIR and SR XRD (Church Of Sant Pere, Terrassa, Spain). *Archaeometry* 52:308–319
- Mairinger F, Schreiner M (1986) Deterioration and preservation of Carolingian and medieval mural paintings in the Münstair Convent (Switzerland)—part II: materials and rendering of the Carolingian wall paintings. In: Bromelle NS, Smith P (eds) *Case studies in the conservation of stone and wall paintings: contributions to the 1986 IIC Congress*. International Institute for Conservation, London, pp 195–196
- Martinelli N, Pignatelli O (2013) Datazione assoluta delle strutture lignee dell'abside. In: De Marchi PM (ed) *Castelseprio e Torba: sintesi delle ricerche e aggiornamenti*. SAP Società Archeologica s.r.l., Mantova, pp 359–563
- Mathieu JR (ed) (2002) *Experimental archaeology, replicating past objects, behaviors and processes*. British Archaeological Reports, Oxford
- Mazzocchin GA, Rudello D, Bragato C, Agnoli F (2004) A short note on Egyptian blue. *J Cult Herit* 5:129–133
- Moezzi A, McDonagh AM, Cortie MB (2012) Zinc oxide particles: synthesis, properties and applications. *Chem Eng J* 185–186:1–22
- Momma K, Izumi F (2011) VESTA 3 for three-dimensional visualization of crystal, volumetric and morphology data. *J Appl Crystallogr* 44:1272–1276
- Nicola M, Aceto M, Gheroldi V, Gobetto R, Chiari G (2018a) Egyptian blue in the Castelseprio mural painting cycle. Imaging and evidence of a non-traditional manufacture. *J Archaeol Sci Rep* 19:465–475
- Nicola M, Musso S, Petacchi S (2018b) Non invasive diagnostic techniques in the authentication and study of Egyptian coffins. The case of the anthropoid coffin of Pakharu, son of Panehesy and the cartonnage of Asetirdis in the Stibbert Museum, Florence. In: Dawson J, Strudwick H (eds) *Ancient Egyptian coffins: past–present–future*. Oxbow Books, pp 121–130
- Onorati G, Conrad G, Michaud L (1987) Identification de deux silicates de cuivre de synthèse, confondus sous l'appellation generique de "bleu égyptien", et définition des ceramiques "bleu antique" retrouvées dans les fresques. *Comptes rendus l'Academie des Sci* 304:651–655
- Pabst A (1959) Structures of some tetragonal sheet silicates. *Acta Crystallogr* 12:733–739
- Pagès-Camagna S, Colinart S, Coupry C (1999) Fabrication processes of archaeological Egyptian blue and green pigments enlightened by Raman microscopy and scanning electronic microscopy. *J Raman Spectrosc* 30:313–317
- Pagès-Camagna S, Colinart S (2003) The Egyptian green pigment: its manufacturing process and links to Egyptian blue. *Archaeometry* 45:637–658
- Pozza G, Ajò D, Chiari G, De Zuane F, Favaro M (2000) Photoluminescence of the inorganic pigments Egyptian blue, Han blue and Han purple. *J Cult Herit* 1:393–398
- Pradell T, Salvado N, Hatton GD, Tite MS (2006) Physical processes involved in production of the ancient pigment, Egyptian blue. *J Am Ceram Soc* 89:1426–1431
- Riederer J (1997) Egyptian blue. In: West Fitzhugh E (ed) *Artists' pigments: a handbook of their history and characteristics*, vol 3. National Gallery of Art, Washington, pp 23–45
- Rigaku Oxford Diffraction (2015) *CrysAlisPro Software System*, Version 1.171, Rigaku Corporation, Oxford, UK
- Salguero TT, Johnson-McDaniel D, Barrett CA (2014) Metal silicate nanosheets, methods of making metal silicate nanosheets, and methods of use. United States Patent no. 9028957
- Sheldrick GM (2008) A short history of SHELX. *Acta Crystallogr A* 64:112–122
- Shortland A, Schachner L, Freestone I, Tite MS (2006) Natron as a flux in the early vitreous materials industry: sources, beginnings and reasons for decline. *J Archaeol Sci* 33:521–530
- Smith GD, Nunan E, Walker C, Kushel D (2009) Inexpensive, near-infrared imaging of artwork using a night-vision webcam for chemistry-of-art courses. *J Chem Educ* 86:1382–1388
- Tian T, Wu C, Chang J (2016) Preparation and in vitro osteogenic, angiogenic and antibacterial properties of cuprorivaite ($\text{CaCuSi}_4\text{O}_{10}$, Cup) bioceramics. *RSC Adv* 6:45840–45849
- Tite MS, Bimson M, Cowell MR (1984) Technological examination of Egyptian blue. In: Lambert J (ed) *Archaeological chemistry III*. American Chemical Society, Washington DC, pp 215–242
- Vettori S, Bracci S, Cantisani E et al (2019) Archaeometric and archaeological study of painted plaster from the Church of St. Philip in Hierapolis of Phrygia (Turkey). *J Archaeol Sci Rep* 24:869–878
- Verri G (2009a) The application of visible-induced luminescence imaging to the examination of museum objects. In: Pezzati L, Salimbeni R (eds) *Proceedings of SPIE 7391, O3A: optics for arts, architecture, and archaeology II*. SPIE Europe Optical Metrology, Munich, p 739105
- Verri G (2009b) The spatially resolved characterisation of Egyptian blue, Han blue and Han purple by photo-induced luminescence digital imaging. *Anal Bioanal Chem* 394:1011–1021
- Vitruvius (1999) In: Rowland I (ed) *Ten books on architecture*. Cambridge University Press, Cambridge
- Warner TE (2011) Artificial cuprorivaite $\text{CaCuSi}_4\text{O}_{10}$ (Egyptian blue) by a salt-flux method. Wiley, Chichester (UK)

Publisher's note Springer Nature remains neutral with regard to jurisdictional claims in published maps and institutional affiliations.